Applied Catalysis B: Environmental 96 (2010) 441–448

Contents lists available at ScienceDirect

Applied Catalysis B: Environmental

journal homepage: www.elsevier.com/locate/apcatb

A comparative study between Co and Rh for steam reforming of ethanol

Ayman M. Karim[a], Yu Su[a], Junming Sun[a], Cheng Yang[b], James J. Strohm[a], David L. King[a], Yong Wang[a,c,*]

[a] Institute for Interfacial Catalysis, Pacific Northwest National Laboratory, Richland, WA 99352, United States
[b] Qingdao Institute of Bioenergy and Bioprocess Technology, Chinese Academy of Sciences, China
[c] The Gene and Linda Voiland School of Chemical Engineering and Bioengineering, Washington State University, Pullman, WA 99164-2710, United States

ARTICLE INFO

Article history:
Received 29 December 2009
Received in revised form 22 February 2010
Accepted 25 February 2010
Available online 6 March 2010

Keywords:
Ethanol reforming
Cobalt catalyst
Rhodium catalyst
Carbon deposition
Reaction pathway

ABSTRACT

Rh and Co-based catalyst performance was compared for steam reforming of ethanol under conditions suitable for industrial hydrogen production. The reaction conditions were varied to elucidate the differences in reaction pathways on both catalysts. On Co/ZnO, CH_4 is a secondary product formed through the methanation reaction, while it is produced directly by ethanol decomposition on Rh. The difference in the reaction pathway is shown to favor Co-based catalysts for selective hydrogen production under elevated system pressures (up to 15 bar) of industrial importance. The carbon deposition rate was also studied, and we show that Co is more prone to coking and catalyst failure. However, the Co/ZnO catalyst can be regenerated, by mild oxidation, despite the high carbon deposition rate. We conclude that Co/ZnO is a more suitable catalyst system for steam reforming of ethanol due to the low methane selectivity, low cost and the possibility of regeneration with mild oxidation.

1. Introduction

Hydrogen is a clean energy carrier and has been considered for use in fuel cells for pollution-free generation of electricity. However, hydrogen is conventionally produced from non-renewable fossil-based feedstocks, primarily through methane steam reforming. Currently, bioethanol, one of the most produced biofuels, is mostly produced from sugarcane, corn and sugar beets [1], however, it can also be produced from lignocellulosic biomass through hydrolysis followed by fermentation [2]. In addition to being produced from renewable sources, bioethanol has high hydrogen content. Autothermal reforming and partial oxidation of ethanol require the use of oxygen, which would increase the operational cost if pure oxygen were used or would complicate and increase the downstream H_2 purification costs, if air were used. Moreover, operation at elevated pressure is preferred from the point of view of hydrogen purification and delivery. Therefore, steam reforming of ethanol, which can generate required pressures through the ability to pump liquids, is considered the preferred method for hydrogen production.

Steam reforming of ethanol has been extensively studied in the last decade [3]. For the process to be commercialized, several issues need to be addressed. Whether the hydrogen produced from steam reforming of ethanol will be used in the chemical industry (e.g. hydrodesulfurization, hydrocracking, NH_3 synthesis . . . etc.) or for direct use in PEM fuel cells or H_2 internal combustion engines, hydrogen purification would be required. Hydrogen purification is typically done through a pressure swing adsorption process which requires that the inlet gas be at high pressure. Additionally, the industrial processes using hydrogen are operated at high pressure (e.g. NH_3 synthesis or hydrocracking). Therefore, for downstream purification and storage, the steam reforming of ethanol process needs to be operated at elevated system pressure. Therefore, catalyst performance, especially selectivity, should be evaluated at elevated pressures. Also, since catalyst coking is an issue during steam reforming of ethanol, catalyst regeneration needs to be studied.

Many catalytic metals and bimetallics (Co, Cu, Ni, Ir, Ru, Pt, Pd, PdZn, Rh, Rh–Pt, Rh–Pd, Rh–Co, Rh–Ni) have been studied for steam reforming of ethanol [4–38]. Of the systems reported in the literature, Rh and Co-based catalysts proved to be the most promising candidates in terms of activity and selectivity to H_2 and CO_2 [25–27,32,33,36–43]. The best catalyst support in the case of Rh was a ceria mixed oxide [33,37] while ZnO was shown to be one of the best oxide supports for Co [42,44]. Despite being extensively studied, a comparative study showing the advantages and limitations of both catalyst systems, under realistic industrial conditions, is lacking. For example, the effect of ethanol partial pressure and S/C ratio on the product distribution has not been systematically studied. Also, to our knowledge, steam reforming of ethanol at high pressure has not been reported. The goal of this work is to pro-

* Corresponding author at: Institute for Interfacial Catalysis, Pacific Northwest National Laboratory, Richland, WA 99352, United States.
E-mail address: yongwang@pnl.gov (Y. Wang).

0926-3373/$ – see front matter © 2010 Elsevier B.V. All rights reserved.
doi:10.1016/j.apcatb.2010.02.041

vide a recommendation of a suitable catalyst, based on either Rh or Co, for the potential commercialization of ethanol reforming. The $Rh/Y_xPr_yCe_{1-x-y}O_2$ and Co/ZnO catalysts are compared based on their activity, selectivity, reaction pathway, deactivation and regeneration. Different catalyst supports for Rh and Co were chosen based on previous reports and our own work, where Ce mixed oxides and ZnO were shown to be the best oxide supports for Rh and Co, respectively [33,37,42,44]. We show that based on the catalyst performance (especially at high pressure) and cost, a Co-based catalyst is superior to Rh, and could be a suitable catalyst system for the commercialization of steam reforming of ethanol.

2. Experimental

2.1. Catalyst synthesis

The ceria mixed oxide supports for the Rh catalysts were prepared by co-precipitation of aqueous solutions of Ce and Zr (and/or Pr and Y) nitrate (98% purity from Sigma–Aldrich). The metal nitrates were dissolved in water and the pH was adjusted by the drop-wise addition of ammonium hydroxide until the pH reached 10. The precipitate was washed with D.I. water, filtered and dried under vacuum overnight. The dried powder was calcined in air at 600 °C for 3 h following a 5 °C/min ramp rate from room temperature. Rh was impregnated on the support by incipient wetness using $Rh(NO_3)_2$ (Sigma–Aldrich) in water. The nominal Rh loading was 2 wt% unless otherwise mentioned. The catalyst was dried at 80 °C then calcined in air at 600 °C for 3 h (5 °C/min ramp rate). More details on the catalyst synthesis regarding the choice of Rh loading and calcination temperature have been reported in our earlier work [32]. Prior to reactivity measurements, the catalyst was reduced in 10% H_2 in N_2 at 350 °C for 1 h following a 2 °C/min temperature ramp from room temperature. Co/ZnO was prepared by co-precipitation of $Co(NO_3)_2$ and $Zn(NO_3)_2$ aqueous solutions by drop-wise addition of Na_2CO_3 until the pH reached a value of 9. The precipitate was washed, filtered and dried under vacuum overnight, then calcined in air at 450 °C for 3 h following a 5 °C/min ramp rate from room temperature. The nominal weight loading was 10 wt% Co. Prior to reactivity measurements, the catalyst was reduced in 10% H_2 in N_2 at 450 °C for 2 h following a 5 °C/min ramp rate from room temperature.

2.2. Catalyst characterization

Multi-point BET and the pore structure were measured by an Autosorb-6 gas sorption system (Quantachrome Corporation), after the samples were degassed overnight at 110 °C. Transmission electron microscopy imaging was conducted on a JEOL 2010 high-resolution analytical electron microscope operating at 200 kV with a LaB_6 filament. Powder samples were mounted on copper grids with lacey carbon support film. Carbon deposition was evaluated by temperature programmed oxidation (TPO) on a LECO RC612 multiphase carbon analyzer. Typically 20 mg of spent catalyst was weighed onto a quartz sample boat and placed in a quartz combustion tube. Under a continuous flow of UHP oxygen, the sample was heated from 100 °C to 1000 °C at 30 °C/min with a final hold time of 10 min. All evolved gases entrained in the oxygen flow were then passed through a copper oxide catalyst bed, held constant at 750 °C to ensure complete combustion to CO_2 and H_2O. CO_2 and H_2O evolution during TPO analysis was continuously monitored with three inline IR cells calibrated and tuned to quantify CO_2 (high and low concentrations) and H_2O on a sample weight basis. Total carbon deposition on the catalyst is defined by the total weight of carbon evolved as CO_2 per weight of catalyst. The measured carbon deposited per gram of catalyst was normalized to the amount of ethanol converted per gram of catalyst (during the entire TOS) to calculate the average carbon deposition rate ($\mu g\,C/g_{EtOH}$ converted).

2.3. Reactivity measurements

The catalytic activity tests were conducted in a 5.2 mm i.d. fixed-bed reactor at pressure ranging from ambient up to 15 bar. The catalyst, diluted with SiC (5× by weight), was loaded between two layers of quartz wool inside the reactor. Two K-type thermocouples were placed in the reactor for the measurement of inlet and catalyst bed temperatures. An Acuflow HPLC pump was used to feed the water/ethanol solution (molar ratio of 10:1, 8:1 or 4:1) and a Brooks Mass Flow Controller (5850E series) was used to control the N_2 flow. The mixture of N_2, water and ethanol was fed to a multichannel vaporizer operating at 160 °C. The ethanol mole fraction in the feed was varied between 2.2% and 10.6% by adjusting the N_2 and water/ethanol flow rates. The effluent of the reactor was analyzed by means of an online Shimadzu GC (Model 2014) equipped with a flame ionization detector (FID) and a HP plot/Q column to quantify the liquid products and the unreacted ethanol. After condensing the liquid products and unreacted water and ethanol, the gas products were analyzed online by means of a MTI Quad Micro GC (Model Q30L) equipped with MS-5A and PPQ columns and two thermals conductivity detectors (TCDs). The catalyst conversion and selectivity are defined on a carbon basis as shown below:

$$\text{Ethanol conversion } (\%) = \frac{\text{moles of ethanol reacted}}{\text{moles of ethanol fed}} \times 100$$

$$\text{Selectivity } (\%) = \frac{\text{moles } P_i \times \upsilon_i}{\text{moles of ethanol reacted} \times 2} \times 100$$

where P_i is a certain product and υ is the number of carbon atoms/molecule in P_i. e.g. if $P = CO_2$, $\upsilon_{CO_2} = 1$, while for $P = CH_3CHO$, $\upsilon_{CH_3CHO} = 2$

2.4. Catalyst regeneration

Following reaction, some Co/ZnO catalyst samples were purged with 100 sccm N_2 then cooled to room temperature under N_2 flow. The samples were then subjected to *in situ* regeneration in 2% O_2 at 400 °C (with a temperature ramp of 10 °C/min) for 1 h. The catalyst was then reduced at 450 °C in 10% H_2 before re-testing for ethanol reforming.

2.5. Thermodynamic equilibrium calculations

The equilibrium product composition at different reaction conditions and reactant composition was calculated by Gibbs free energy minimization using the software package HSC Chemistry version 6.12 (Outotec Research Oy, Pori Finland).

3. Results

3.1. Reaction pathway

The desired products from steam reforming of ethanol (reaction (1)) are H_2 and CO_2. However, due to a complex reaction network [45], several by-products can be formed on the metal and/or support, e.g. CH_4, CO, C_2H_4, CH_3CHO. C_2H_4 is a highly undesired product since it is a precursor to coke and will lead to fast catalyst deactivation [46,47]. CH_4 production lowers the selectivity to H_2 and a downstream CH_4 reformer would be required, which increases the capital and operational costs. Minimization of by-product formation is essential in achieving high H_2 selec-

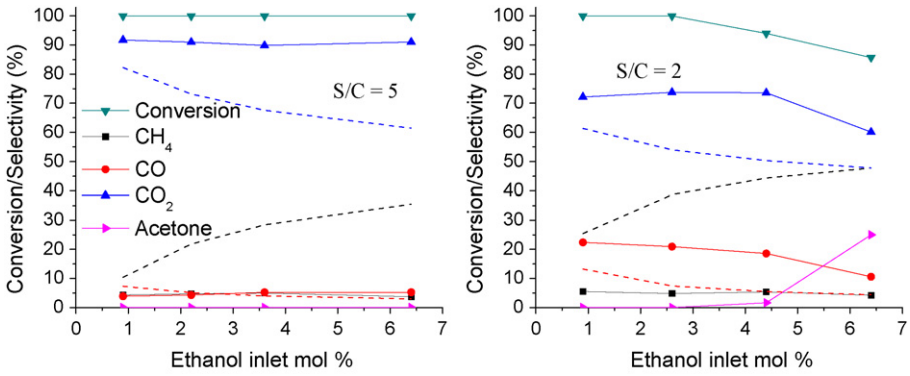

Fig. 1. Effect of S/C ratio and ethanol partial pressure on the selectivity of 10% Co/ZnO during steam reforming of ethanol. $T = 450\,^{\circ}C$, $P = 7$ psig, GHSV = 18,000 h^{-1}. Dashed lines represent the equilibrium selectivity of CH_4 (black), CO (red) and CO_2 (blue) (For interpretation of the references to color in this figure legend, the reader is referred to the web version of the article.).

tivity, increasing catalyst stability and lowering the downstream processing for H_2 purification.

The effect of S/C ratio and ethanol partial pressure on the activity and selectivity of 10% Co/ZnO catalyst is shown in Fig. 1. It can be seen that under all the conditions studied, CO_2 and CH_4 selectivities were above and below their equilibrium values, respectively. CH_4 can be formed by either ethanol decomposition (reaction (4)) or CO/CO_2 methanation (reactions (2) and (3)). Lower than equilibrium CH_4 selectivity suggests that either the ethanol decomposition pathway is slow relative to the reforming pathway or that CH_4 is mainly formed as a secondary product by methanation. The S/C ratio should be expected to affect the methanation of CO/CO_2 (reactions (2) and (3)), however, the CH_4 selectivity was almost independent of the S/C ratio, as shown in Fig. 1. Also, at lower S/C ratio, the CH_4 selectivity was not affected by the increase in CO selectivity. This suggests that, at atmospheric pressure, CH_4 is mainly produced directly by ethanol decomposition (at a much lower rate relative to ethanol reforming) rather than by methanation of CO/CO_2. However, we will show below that at higher system pressure, methanation becomes the major pathway for CH_4 formation on Co/ZnO.

$$C_2H_5OH + 3H_2O \rightarrow 2CO_2 + 6H_2 \quad (1)$$

$$CO + 3H_2 \leftrightarrow CH_4 + H_2O \quad (2)$$

$$CO_2 + 4H_2 \leftrightarrow CH_A + 2H_2O \quad (3)$$

$$C_2H_5OH \rightarrow CO + CH_4 + H_2 \quad (4)$$

$$CO + H_2O \leftrightarrow CO_2 + H_2 \quad (5)$$

Higher than equilibrium CO_2 selectivity could be incorrectly attributed to CO_2 being a primary product, however, since the selectivity to CH_4 is very low, the equilibrium for the water gas shift (reaction (5)) needs to be considered instead of the overall equilibrium. The ratio $[CO_2][H_2]/[CO][H_2O]$ was calculated for the different conditions in Fig. 1 using the measured gas phase composition (water was estimated from products composition and ethanol conversion). The ratio was compared to the equilibrium constant for water gas shift (WGS), K_p and the results indicated that $[CO_2][H_2]/[CO][H_2O] \times 1/K_p$ was ~1 (±20%) under all the experimental conditions in Fig. 1. Therefore, determining whether CO_2 is a primary or secondary product is not possible from the data in Fig. 1. In other experiments (not shown), the gas residence time was varied over a wider range and the $[CO_2][H_2]/[CO][H_2O] \times 1/K_p$ ratio was observed to decrease from ~1 at longer residence time to about 0.2 at shorter residence time. These results indicate that CO is a primary product on Co/ZnO while CO_2 is formed through the WGS reaction. Small amounts of Co added to Fe-based high temperature water gas shift catalysts have been shown to enhance the activity [48]. We can conclude that the WGS rate is very fast, resulting in high selectivity to CO_2 (subject to WGS equilibrium constraint).

In contrast to Co/ZnO, $Rh/Y_{0.1}Pr_{0.2}Ce_{0.7}O_2$ exhibited a much higher selectivity to CH_4, as shown in Fig. 2a. It can also be seen that CH_4 selectivity increased significantly with the increase in ethanol partial pressure. However, CH_4 selectivity was not consistently above or below the equilibrium value at different ethanol

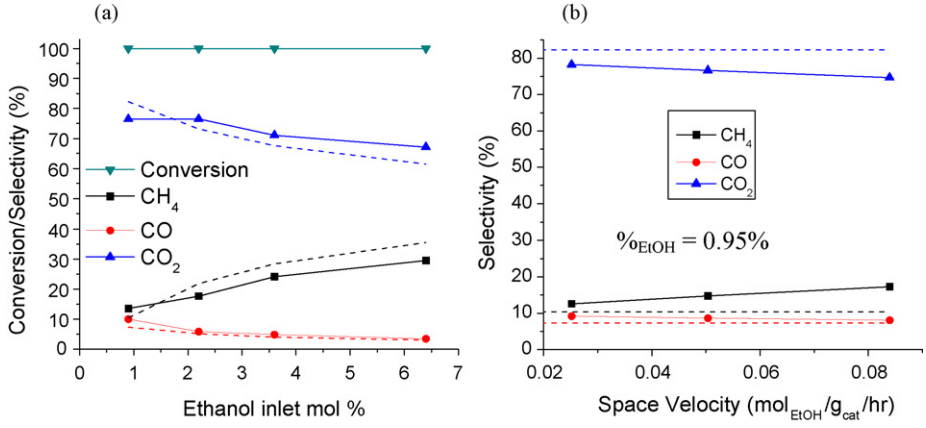

Fig. 2. Effect of (a) ethanol partial pressure and (b) space velocity on the selectivity of 2.3% $Rh/Y_{0.1}Pr_{0.2}Ce_{0.7}O_2$ during steam reforming of ethanol. $T = 450\,^{\circ}C$, S/C = 5, $P = 7$ psig, (a) GHSV = 18,000 h^{-1} and (b) Ethanol inlet mol% = 0.95%. Ethanol conversion was 100% under all conditions. Dashed lines represent the equilibrium selectivity of CH_4 (black), CO (red) and CO_2 (blue) (For interpretation of the references to color in this figure legend, the reader is referred to the web version of the article.).

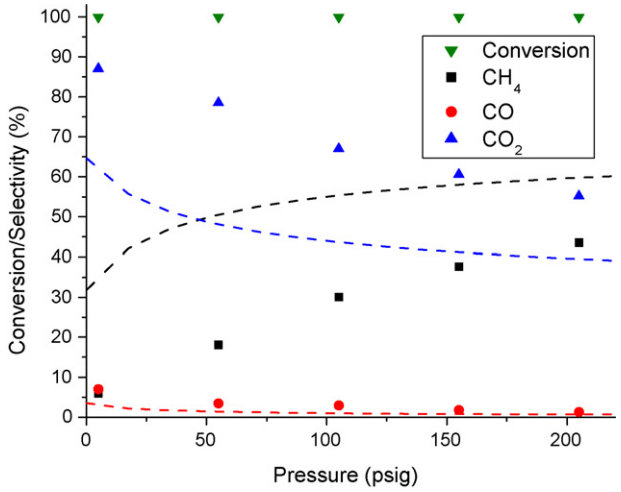

Fig. 3. 10% Co/ZnO catalyst activity and selectivity for steam reforming of ethanol as a function of total system pressure. Dashed lines represent the equilibrium selectivity of CH_4 (black), CO (red) and CO_2 (blue). Reaction conditions: T = 450 °C, S/C = 5, GHSV, = 11,000 h^{-1}, Ethanol inlet mol% = 4.7%, catalyst diluted with SiC 5× by weight (For interpretation of the references to color in this figure legend, the reader is referred to the web version of the article.).

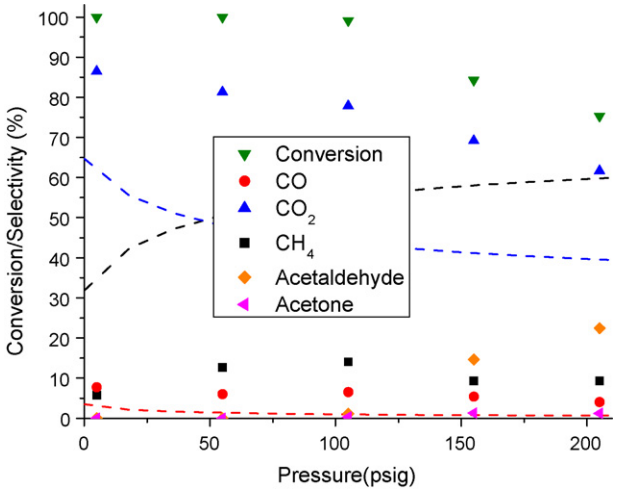

Fig. 5. 10% Co/ZnO catalyst activity and selectivity for steam reforming of ethanol as a function of total system pressure at constant residence time. Dashed lines represent the equilibrium selectivity of CH_4 (black), CO (red) and CO_2 (blue). Reaction conditions: T = 450 °C, S/C = 5, GHSV, = 11,000–77,600 h^{-1}, Ethanol inlet mol% = 4.7%, catalyst diluted with SiC 5× by weight (For interpretation of the references to color in this figure legend, the reader is referred to the web version of the article.).

partial pressures, but seemed to track the equilibrium line. In order to determine the reaction pathway for CH_4 formation, the space velocity was varied while maintaining the ethanol partial pressure constant at 0.0095 atm as shown in Fig. 2b. CH_4 selectivity increased at higher space velocities indicating that CH_4 is a primary product on $Rh/Y_{0.1}Pr_{0.2}Ce_{0.7}O_2$. Analysis of the approach to WGS equilibrium $[CO_2][H_2]/[CO][H_2O] \times 1/K_p$ under the different conditions in Fig. 2 revealed that CO_2 is a secondary product formed by the WGS reaction similar to Co/ZnO. Therefore, the reaction pathway for ethanol reforming on Rh is through the decomposition of ethanol, followed by methane reforming and water gas shift. This is in agreement with previous work on Rh/CeO_2 [49].

3.2. Effect of reaction pressure on selectivity

As mentioned in the introduction, downstream purification and storage requires high pressure operation of the ethanol reforming.

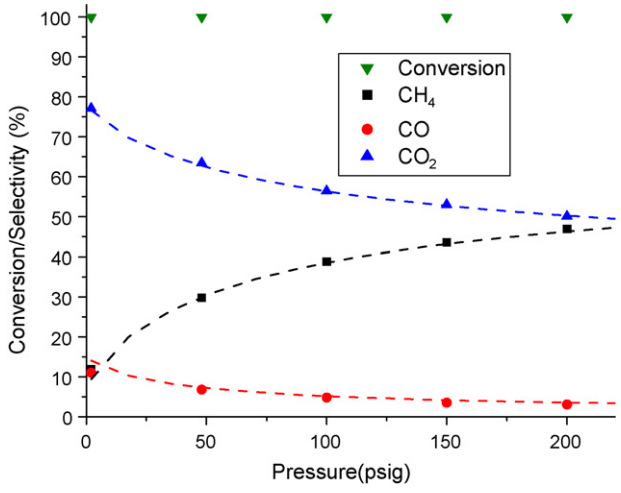

Fig. 4. 2.3% $Rh/Y_{0.1}Pr_{0.2}Ce_{0.7}O_2$ catalyst activity and selectivity for steam reforming of ethanol as a function of total system pressure. Dashed lines represent the equilibrium selectivity of CH_4 (black), CO (red) and CO_2 (blue). Reaction conditions: T = 550 °C, GHSV = 25,000 h^{-1}, S/C = 4, Ethanol inlet mol% = 7.2%, catalyst diluted with SiC 5× by weight, reduction in 10% H_2 at 350 °C, 1 h (For interpretation of the references to color in this figure legend, the reader is referred to the web version of the article.).

In this section, the effect of system pressure on the performance of Co and Rh catalysts for steam reforming of ethanol will be described. The equilibrium CH_4 selectivity increases with pressure (black dashed line in Fig. 3), therefore, it is a requirement that a catalyst provide CH_4 selectivity lower than equilibrium in order to avoid costly downstream CH_4 reforming. Figs. 3 and 4 show the effect of system pressure on the selectivity of Co/ZnO and $Rh/Y_{0.1}Pr_{0.2}Ce_{0.7}O_2$, respectively. As expected, higher pressures lead to higher methane selectivity on both catalysts. However, the CH_4 selectivity on Co/ZnO was still under the equilibrium value at all pressures as shown in Fig. 3. On $Rh/Y_{0.1}Pr_{0.2}Ce_{0.7}O_2$ (Fig. 4), CH_4 selectivity was nearly equal to the equilibrium value at all pressures, which was expected at this low space velocity. As discussed above, ethanol decomposition is the major reaction for CH_4 formation on Rh and the rate increases with higher ethanol partial pressure. Therefore, high CH_4 selectivity (close to equilibrium) would always be attained on Rh at elevated system pressures, regardless of space velocity. The CH_4 selectivity on Co/ZnO at different pressures was lower than equilibrium, suggesting that increasing the space velocity could further lower the CH_4 forma-

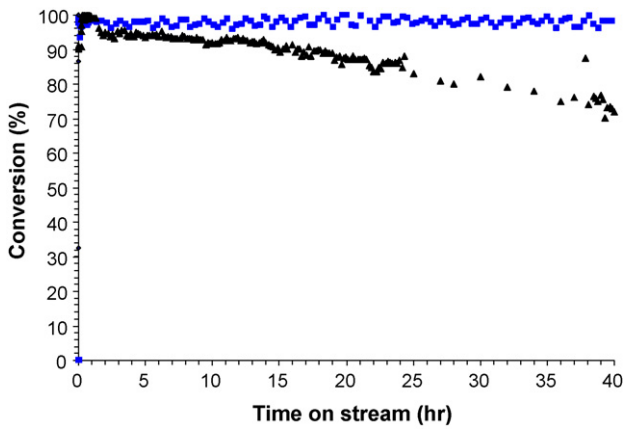

Fig. 6. Effect of support on catalyst stability, 2% $Rh/Ce_{0.8}Zr_{0.2}O_2$ (black triangles) and 2% $Rh/Ce_{0.8}Pr_{0.2}O_2$ (blue squares). Reaction conditions: T = 550 °C, P = 7 psig, S/C = 4, GHSV = 480,000 h^{-1}, $\%_{EtOH}$ = 5.6%, catalyst diluted with SiC 5× by weight, reduction in 10% H_2 at 350 °C, 1 h (For interpretation of the references to color in this figure legend, the reader is referred to the web version of the article.).

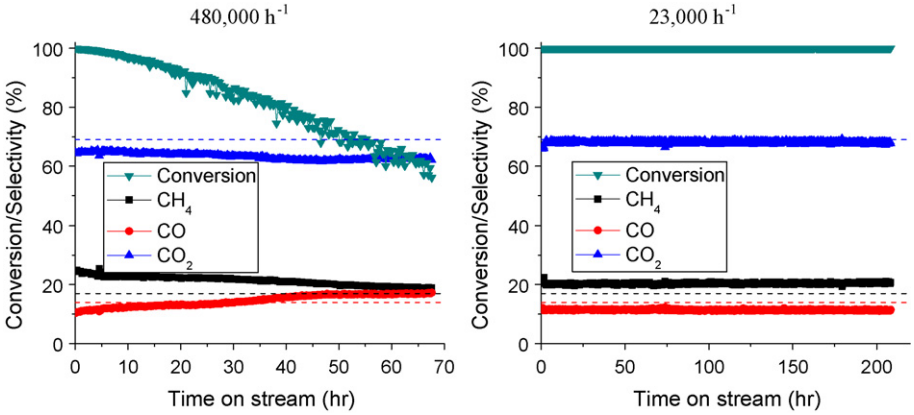

Fig. 7. Effect of space velocity on 2.3% $Rh/Y_{0.1}Pr_{0.2}Ce_{0.7}O_2$ catalyst stability for steam reforming of ethanol. Dashed lines represent the equilibrium selectivity of CH_4 (black), CO (red) and CO_2 (blue) (For interpretation of the references to color in this figure legend, the reader is referred to the web version of the article.).

tion, if methanation is the major pathway for CH_4 formation. Fig. 5 shows the effect of maintaining the gas residence time constant (by increasing the total flowrate) while increasing the system pressure. It can be seen that CH_4 selectivity is significantly reduced by increasing the space velocity, which confirms our hypothesis that CH_4 is mainly formed by methanation on Co/ZnO (the ethanol decomposition pathway contribution to CH_4 formation is small). A similar experiment, where the gas residence time was kept constant, was conducted on the 2.3% $Rh/Y_{0.1}Pr_{0.2}Ce_{0.7}O_2$ catalyst (not shown) and the selectivity was almost unchanged from that in Fig. 4. Therefore, in agreement with the above discussion of Figs. 1 and 2, we can conclude that CH_4 is a primary product on $Rh/Y_{0.1}Pr_{0.2}Ce_{0.7}O_2$, while it is formed indirectly through the methanation of CO/CO_2 on Co/ZnO. The difference in reaction pathway therefore favors the use of Co/ZnO at high pressure in order to achieve high selectivity to hydrogen.

3.3. Catalyst deactivation

Carbon deposition is considered to be the main cause for Rh and Co-based catalyst deactivation in steam reforming of ethanol [47,50,51]. Catalyst supports with high oxygen mobility and oxygen storage capacity help minimize carbon deposition [47,50,51]. The effect of catalyst support on the activity and selectivity of Rh has been studied and it was shown that a high oxygen mobility support, e.g. Ce-Zr mixed oxide, exhibited the highest activity and selectivity to H_2 and CO_2 [32,33,37]. Fig. 6 shows that replacing Zr in $Rh/Ce_{0.8}Zr_{0.2}O_2$ with Pr resulted in higher catalyst stability. Replacing Zr by Pr was reported to increase the oxygen mobility and oxygen storage capacity of the support [52], which could help minimize the carbon deposition [5,53], hence leading to slower deactivation. Despite the higher stability of $Rh/Ce_{0.8}Pr_{0.2}O_2$ catalyst, carbon deposition cannot be completely suppressed, rather catalyst deactivation can only be slowed down. Space velocity has a large impact on catalyst stability, as shown in Fig. 7. At high space velocity (480,000 h^{-1}) the ethanol conversion starts to drop below 100% after 5 h on stream. Five hours on stream at the high space velocity (480,000 h^{-1}) is equivalent (in terms of ethanol fed) to about 104 h at the lower space velocity (23,000 h^{-1}). Therefore, if the lower space velocity is just prolonging the catalyst lifetime due to lower WHSV ($g_{EtOH}/g_{cat}/h$), the ethanol conversion should drop below 100% at about 104 h on stream. However, as seen in Fig. 7, the ethanol conversion is 100% up to 200 h on stream. Also, the catalyst selectivity remains unchanged at the low space velocity, whereas at the high space velocity, the selectivity to CO and CH_4 were not stable from the beginning of the run. These results indicate that lower space velocity results in a more stable catalyst. The higher stability could be due to lower carbon deposition.

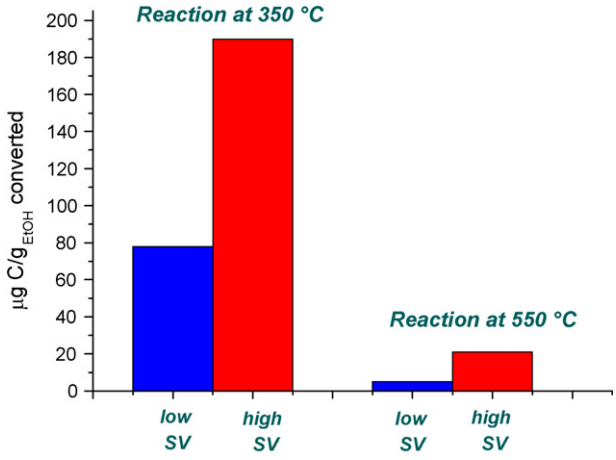

Fig. 8. Effect of reaction temperature and space velocity (low SV = 23,000 h^{-1}, high SV = 480,000 h^{-1}) on carbon deposition rate during steam reforming of ethanol on 2.3% $Rh/Y_{0.1}Pr_{0.2}Ce_{0.7}O_2$. Reaction conditions: P = 7 psig, S/C = 4, $\%_{EtOH}$ = 10.6%, catalyst diluted with SiC 5× by weight, reduction in 10% H_2 at 350 °C, 1 h. Similar amount of ethanol was fed to all catalysts.

In order to confirm our hypothesis, we measured the carbon deposition rate (μg C/g_{EtOH} converted) at different space velocities and temperatures and the results are shown in Fig. 8. It can be seen that higher space velocity and lower reaction temperature favor carbon deposition. Therefore, we can conclude that higher reaction temperatures and lower space velocities are required to minimize the carbon deposition rate on Rh and increase the catalyst stability during steam reforming of ethanol. High carbon deposition rate at low reaction temperatures could be due to the lower oxygen mobility of the support at lower temperature [54]. Ethanol steam reforming test under the same conditions in Fig. 6 (480,000 h^{-1}) was performed on the $Ce_{0.8}Pr_{0.2}O_2$ support and the support exhibited high selectivity to acetone and acetaldehyde and exhibited very fast deactivation in the first hour on stream (not shown). It is known that basic sites promote the formation of acetone from acetaldehyde through an aldol condensation-dehydrogenation reaction pathway [55]. Aldol condensation of acetone could easily proceed on the basic sites to form oligomers which transform into carbon deposits and block the active sites for ethanol reforming [5,56]. In co-feeding experiments, acetone and acetaldehyde have been shown to increase the deactivation rate and lower the catalyst activity, respectively [50]. Therefore, the lower carbon deposition

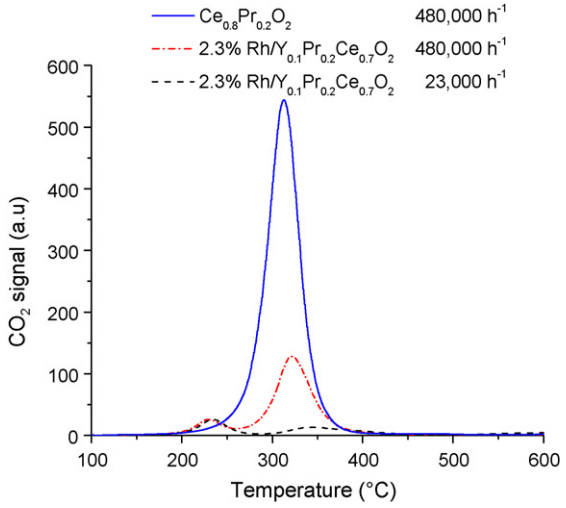

Fig. 9. Temperature programmed oxidation on the spent catalysts. Reaction conditions: $P = 7$ psig, S/C = 4, $\%_{EtOH} = 10.6\%$, catalyst diluted with SiC 5× by weight, reduction in 10% H_2 at 350 °C, 1 h. Similar amount of ethanol was fed to all catalysts.

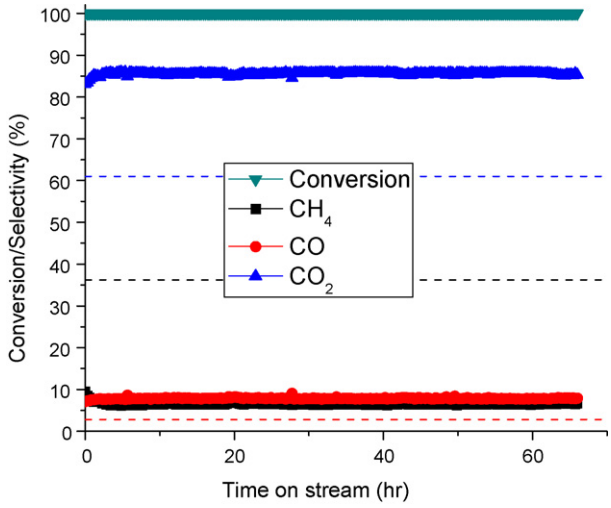

Fig. 10. 10% Co/ZnO catalyst stability for steam reforming of ethanol. Dashed lines represent the equilibrium selectivity of CH_4 (black), CO (red) and CO_2 (blue). Reaction conditions: $T = 450$ °C, $P = 7$ psig, S/C = 5, GHSV = 24,000 h^{-1}, $\%_{EtOH} = 6.6\%$, catalyst diluted with SiC 5× by weight, reduction in 10% H_2 at 450 °C, 1 h (For interpretation of the references to color in this figure legend, the reader is referred to the web version of the article.).

at lower space velocity could be explained using the following simplified argument: ethanol dehydrogenation to acetaldehyde is a relatively fast reaction and could proceed on the support or on Rh. At high space velocity, the acetaldehyde intermediate could accumulate on the catalyst surface due to lower activity for C–C cleavage relative to ethanol dehydrogenation activity. Acetaldehyde could further react to form acetone on the basic sites of the Ce mixed oxide. Also, the coke formation reaction kinetic order in acetaldehyde (and acetone) may be higher than that for reforming (acetaldehyde to CH_4, CO, and CO_2). Therefore, accumulation of acetaldehyde (at higher space velocity) could favor coke formation.

A comparison of the TPO profiles for the spent $Ce_{0.8}Pr_{0.2}O_2$ support and the $Rh/Y_{0.1}Pr_{0.2}Ce_{0.7}O_2$ catalyst, both tested at a space velocity of 480,000 h^{-1} and 550 °C, is shown in Fig. 9. Two CO_2 peaks at 230 °C and 323 °C were observed for the $Rh/Y_{0.1}Pr_{0.2}Ce_{0.7}O_2$, while only a single broad peak centered at 315 °C was observed for the $Ce_{0.8}Pr_{0.2}O_2$ support. The total carbon deposited on the $Ce_{0.8}Pr_{0.2}O_2$ support (710 μg C/g_{EtOH} converted) was much higher than on the $Rh/Y_{0.1}Pr_{0.2}Ce_{0.7}O_2$ (21 μg C/g_{EtOH} converted) in agreement with the faster deactivation on the former. Also shown in Fig. 9 is the TPO profile for $Rh/Y_{0.1}Pr_{0.2}Ce_{0.7}O_2$ tested at a lower space velocity (23,000 h^{-1}). The higher temperature CO_2 peak is smaller for the catalyst tested at a lower space velocity while the low temperature peak is similar in intensity to the catalyst tested at 480,000 h^{-1}. The CO_2 peak at high temperature could be assigned to the carbon deposited on the Rh-support interface and on the support. The intensity of the CO_2 peak at high temperature decreased in the order $Ce_{0.8}Pr_{0.2}O_2$ (480,000 h^{-1}) > $Rh/Y_{0.1}Pr_{0.2}Ce_{0.7}O_2$ (480,000 h^{-1}) > $Rh/Y_{0.1}Pr_{0.2}Ce_{0.7}O_2$ (23,000 h^{-1}). Acetaldehyde and acetone selectivity was highest on $Ce_{0.8}Pr_{0.2}O_2$ which supports our hypothesis that accumulation of acetaldehyde and acetone results in fast carbon deposition.

Co/ZnO showed stable performance for up to 65 h (see Fig. 10), however significant carbon deposition was observed on the spent catalyst. Fig. 11 shows HRTEM images of the 10% Co/ZnO and 2.3% $Rh/Y_{0.1}Pr_{0.2}Ce_{0.7}O_2$ catalysts after exposure to steam reforming of ethanol for over 60 h. Co/ZnO shows carbon build-up mostly in the form of filaments forming on the Co particles, while the carbon on $Rh/Y_{0.1}Pr_{0.2}Ce_{0.7}O_2$ appears to be more of an amorphous film covering both the support and metal particles. The BET surface areas for the fresh and spent catalysts are reported in Table 1. The surface area for the spent Co/ZnO catalyst increased while it decreased for the spent $Rh/Y_{0.1}Pr_{0.2}Ce_{0.7}O_2$ catalyst compared to that of the fresh catalysts. This is in agreement with the type of carbon seen in Fig. 11, i.e., carbon filaments are expected to increase the BET surface area of the Co/ZnO catalyst, while amorphous carbon covering the support and Rh particles would plug the pores and decrease the surface area. Table 2 shows the carbon deposition rate results (μg C/g_{EtOH} converted) calculated by normalizing the measured weight of carbon deposited per gram of catalyst by the weight of ethanol converted per gram of catalyst. The normalized results in Table 2 show that the carbon deposition rate on Co/ZnO is two orders of magnitude higher than that on $Rh/Y_{0.1}Pr_{0.2}Ce_{0.7}O_2$. The high carbon deposition rate on Co is not a surprise since, under

Table 1
BET surface area for the fresh and spent catalysts.

Catalyst	BET surface area (m^2/g) Calcined	Spent
2.3% $Rh/Y_{0.1}Pr_{0.2}Ce_{0.7}O_2$ $T = 550$ °C, S/C = 5, $\%_{EtOH} = 10.6\%$	25	12
10% Co/ZnO $T = 450$ °C, S/C = 4, $\%_{EtOH} = 6.6\%$	45	112

Table 2
Carbon deposition rate on 10% Co/ZnO and 2.3% $Rh/Y_{0.1}Pr_{0.2}Ce_{0.7}O_2$ catalysts, space velocity = 24,000 h^{-1} and 23,000 h^{-1}, respectively.

Catalyst	Time on stream	μg C/g_{EtOH} converted
2.3% $Rh/Y_{0.1}Pr_{0.2}Ce_{0.7}O_2$ $T = 550$ °C, S/C = 5, $\%_{EtOH} = 10.6\%$	65	5
10% Co/ZnO $T = 450$ °C, S/C = 4, $\%_{EtOH} = 6.6\%$	40	900

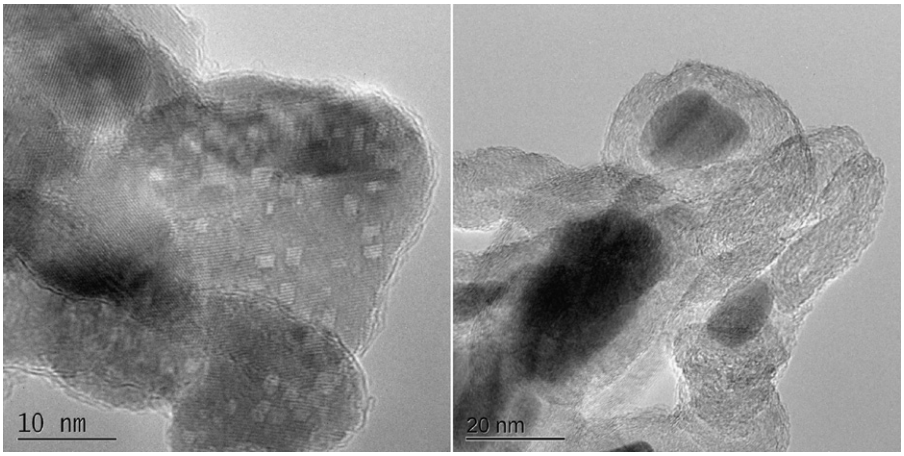

Fig. 11. HRTEM images of the 2.3% $Rh/Y_{0.1}Pr_{0.2}Ce_{0.7}O_2$ (left) and 10% Co/ZnO (right) spent catalysts.

certain reaction conditions, Co was reported to be good catalyst for carbon nanofiber formation, similar to Ni [57]. Carbon filaments were also detected on Co/ZrO_2 during steam reforming of ethanol [51], on Co/Al_2O_3 by CO disproportionation [58], and on Co/SiO_2 during methane decomposition [57,59]. Carbon nanofiber formation on Ni has been reported [60] to occur by the initial formation of carbon atoms on the metal surface followed by dissolution of the carbon atoms in the metal particle. The dissolved carbon atoms diffuse through (or on the surface, around) the metal particle to the support where they are deposited as a graphite layer. This causes the metal particle to detach from the support and the filament continues to grow by the same mechanism. This leaves most of the metal particle free of carbon and therefore could explain why the Co/ZnO catalyst remains active, if the mechanism is similar to that over Ni. However, carbon filaments will eventually cause pressure build-up and significant changes in the catalyst structure. These structural changes could be irreversible (detachment of the Co particles from the support and/or pore plugging), leading to catalyst failure [61]. Regeneration of the Co/ZnO catalyst will likely need to be performed more frequently than for Rh-based catalysts in order to prevent irreversible structural changes caused by the carbon filament formation.

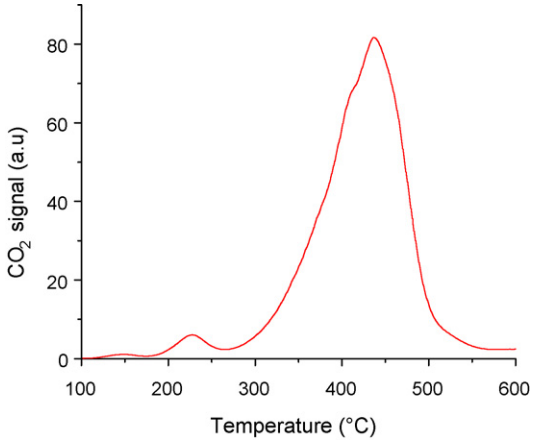

Fig. 12. Temperature programmed oxidation on the 10% Co/ZnO spent catalyst. Reaction conditions: $T = 450\,^{\circ}C$, $P = 7$ psig, S/C = 5, GHSV = 24,000 h^{-1}, $\%_{EtOH} = 6.6\%$, catalyst diluted with SiC 5× by weight, reduction in 10% H_2 at 450 °C, 1 h.

3.4. Catalyst regeneration

Rh-based catalyst activity and selectivity has been shown to be restored by oxidation under mild conditions followed by reduction [47]. This is attributed to the easy burn-off of the amorphous type of carbon deposited on the catalyst during reaction. Co/ZnO showed stable performance for up to 65 h (see Fig. 10), however, there was a significant carbon deposition as shown in Table 1 and in the HRTEM image in Fig. 11. Also, since the conversion in Fig. 10 was 100%, catalyst deactivation cannot be excluded during the 65 h of operation, and it is expected that the Co/ZnO catalyst will eventually deactivate due to carbon deposition. The main challenge would be to find methods to remove the deposited carbon filaments and restore the original catalyst activity and selectivity. Catalyst regeneration by oxidation at 400 °C was chosen based on the temperature programmed oxidation profile for a spent 10% Co/ZnO catalyst (see Fig. 12). Fig. 13 shows the Co/ZnO catalyst performance after the long term catalytic test (see Fig. 9) and subsequent regeneration at 400 °C in 2% O_2 followed by reduction in 10% H_2 at 450 °C. The regenerated Co/ZnO catalyst activity and selectivity were similar to that of the fresh catalyst (Fig. 10) and it was stable up to 65 h. However, starting at around TOS = 30 h, small amounts of acetaldehyde and acetone (selectivity less than 3% and 1%, respectively at TOS = 65 h) were detected. Consequently, the selectivity to CO_2

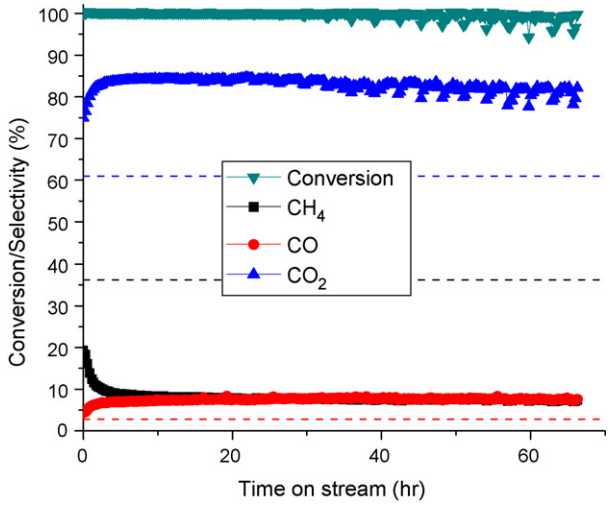

Fig. 13. Regenerated 10% Co/ZnO catalyst stability for steam reforming of ethanol. Regeneration was performed in 100 sccm flow of 2% O_2 in He at 400 °C for 1 h, followed by reduction in 10% H_2 at 450 °C for 1 h. Dashed lines represent the equilibrium selectivity of CH_4 (black), CO (red) and CO_2 (blue). Reaction conditions: $T = 450\,^{\circ}C$, $P = 7$ psig, S/C = 5, GHSV = 24,000 h^{-1}, $\%_{EtOH} = 6.6\%$, catalyst diluted with SiC 5× by weight (For interpretation of the references to color in this figure legend, the reader is referred to the web version of the article.).

slightly decreased from 84% at the beginning to 81% towards the end of the run. The detection of liquid products (acetaldehyde and acetone) and the drop in ethanol conversion to about 98% indicate a reduction in catalyst activity after regeneration, compared with the fresh catalyst. This suggests that there could be a maximum number of regeneration cycles before the catalyst performance could not be recovered for long enough time. Optimization of the regeneration procedure and frequency to prolong the catalyst life is beyond the scope of this work. Our results show that regeneration of Co/ZnO is possible if performed before a substantial change in the catalyst structure occurs. On the other hand, in other experiments (not shown) where the fresh catalyst was kept on stream until the conversion dropped to about 70%, the catalyst activity and selectivity could not be restored by regeneration.

4. Conclusions

We have shown that the reaction pathway for ethanol reforming is different on Co and Rh. On Co/ZnO, CH_4 is a secondary product formed through the methanation of CO and/or CO_2. In contrast, CH_4 is produced by direct ethanol decomposition on Rh. The selectivity to CH_4 on Rh approaches thermodynamic equilibrium, which at high pressures favors high CH_4 selectivity. The Co and Rh catalyst performances were investigated at high reaction pressures (up to 15 bar) and Co was much more selective to CO_2 and H_2 than Rh, in agreement with the proposed difference in reaction pathway. Both catalyst systems showed carbon deposition, however, the rate for carbon deposition on Co was two orders of magnitude higher than Rh. Despite this high carbon deposition rate, we have demonstrated the possibility of Co/ZnO catalyst regeneration. We conclude that Co/ZnO is a more suitable catalyst system for steam reforming of ethanol due to its lower methane selectivity and lower cost, along with the possibility that the necessary regeneration can be accomplished with mild oxidation. However, further work is required to identify methods to mitigate carbon formation on the Co/ZnO and study the effect of multiple regeneration cycles and frequency of regeneration on the catalyst performance and lifetime.

Acknowledgments

The authors would like to thank the U.S. Department of Energy, Office of Energy Efficiency and Renewable Energy, for financial support of this work. A portion of the research was performed using the Environmental Molecular Sciences Laboratory, a national scientific user facility sponsored by the Department of Energy's Office of Biological and Environmental Research located at Pacific Northwest National Laboratory.

References

[1] L. Hernández, V. Kafarov, International Journal of Hydrogen Energy 34 (2009) 7041–7050.
[2] C.N. Hamelinck, G.V. Hooijdonk, A.P.C. Faaij, Biomass and Bioenergy 28 (2005) 384–410.
[3] M. Ni, D.Y.C. Leung, M.K.H. Leung, International Journal of Hydrogen Energy 32 (2007) 3238–3247.
[4] B.C. Zhang, X.L. Tang, Y. Li, Y.D. Xu, W.J. Shen, International Journal of Hydrogen Energy 32 (2007) 2367–2373.
[5] B.C. Zhang, X.L. Tang, Y. Li, W.J. Cai, Y.D. Xu, W.J. Shen, Catalysis Communications 7 (2006) 367–372.
[6] B.C. Zhang, Y. Li, W.J. Cai, X.L. Tang, Y.D. Xu, W.J. Shen, Chinese Journal of Catalysis 27 (2006) 567–572.
[7] M.H. Youn, J.G. Seo, P. Kim, I.K. Song, Journal of Molecular Catalysis A: Chemical 261 (2007) 276–281.
[8] M.H. Youn, J.G. Seo, K.M. Cho, J.C. Jung, H. Min, K.W. La, D.R. Park, S. Park, S.H. Lee, I.K. Song, Korean Journal of Chemical Engineering 25 (2008) 236–238.
[9] Y. Yang, F. Wu, J.X. Ma, Chinese Journal of Catalysis 26 (2005) 131–137.
[10] Y. Yang, J.X. Ma, F. Wu, International Journal of Hydrogen Energy 31 (2006) 877–882.
[11] L. Wang, S.Q. Chen, Y. Liu, Acta Physico-Chimica Sinica 24 (2008) 849–854.
[12] H. Wang, J.L. Ye, Y. Liu, Y.D. Li, Y.N. Qin, Catalysis Today 129 (2007) 305–312.
[13] H. Wang, P.X. Liu, Y. Liu, Y.N. Qin, Chinese Journal of Catalysis 27 (2006) 976–982.
[14] E.C. Wanat, K. Venkataraman, L.D. Schmidt, Applied Catalysis A: General 276 (2004) 155–162.
[15] A.J. Vizcaino, A. Carriero, J.A. Calles, International Journal of Hydrogen Energy 32 (2007) 1450–1461.
[16] P.D. Vaidya, A.E. Rodrigues, Industrial & Engineering Chemistry Research 45 (2006) 6614–6618.
[17] K. Urasaki, K. Tokunaga, Y. Sekine, M. Matsukata, E. Kikuchi, Catalysis Communications 9 (2008) 600–604.
[18] K. Urasaki, K. Tokunaga, Y. Sekine, E. Kikuchi, M. Matsukata, Chemistry Letters 34 (2005) 668–669.
[19] S. Tuti, F. Pepe, Catalysis Letters 122 (2008) 196–203.
[20] J. Sun, F. Wu, X.P. Qiu, F. Wang, S.J. Hao, Y. Liu, Chinese Journal of Catalysis 25 (2004) 551–555.
[21] J. Sun, X.P. Qiu, F. Wu, W.T. Zhu, W.D. Wang, S.J. Hao, International Journal of Hydrogen Energy 29 (2004) 1075–1081.
[22] J. Sun, X.P. Qiu, F. Wu, W.T. Zhu, International Journal of Hydrogen Energy 30 (2005) 437–445.
[23] J. Sun, D.F. Luo, P. Xiao, J.G. Li, S. Yu, Journal of Power Sources 184 (2008) 385–391.
[24] D. Srinivas, C.V.V. Satyanarayana, H.S. Potdar, P. Ratnasamy, Applied Catalysis A: General 246 (2003) 323–334.
[25] H. Song, L.Z. Zhang, U.S. Ozkan, Green Chemistry 9 (2007) 686–694.
[26] P.Y. Sheng, W.W. Chiu, A. Yee, S.J. Morrison, H. Idriss, Catalysis Today 129 (2007) 313–321.
[27] M. Scott, M. Goeffroy, W. Chiu, M.A. Blackford, H. Idriss, Topics in Catalysis 51 (2008) 13–21.
[28] R.K.S. Santos, M.S. Batista, E.M. Assaf, J.M. Assaf, Quimica Nova 28 (2005) 587–590.
[29] M.C. Sanchez-Sanchez, R.M. Navarro, J.L.G. Fierro, International Journal of Hydrogen Energy 32 (2007) 1462–1471.
[30] M.C. Sanchez-Sanchez, R.M. Navarro, J.L.G. Fierro, Catalysis Today 129 (2007) 336–345.
[31] M.C. Sanchez-Sanchez, R. Navarro, J.L.G. Fierro, Abstracts of Papers of the American Chemical Society 231 (2006).
[32] H.S. Roh, Y. Wang, D.L. King, A. Platon, Y.H. Chin, Catalysis Letters 108 (2006) 15–19.
[33] H.S. Roh, Y. Wang, D.L. King, Topics in Catalysis 49 (2008) 32–37.
[34] J. Rasko, A. Hancz, A. Erdohelyi, Applied Catalysis A: General 269 (2004) 13–25.
[35] L.P.R. Profeti, E.A. Ticianelli, E.M. Assaf, Journal of Power Sources 175 (2008) 482–489.
[36] P.Y. Sheng, A. Yee, G.A. Bowmaker, H. Idriss, Journal of Catalysis 208 (2002) 393–403.
[37] C. Diagne, H. Idriss, K. Pearson, M.A. Gomez-Garcia, A. Kiennemann, Comptes Rendus Chimie 7 (2004) 617–622.
[38] C. Diagne, H. Idriss, A. Kiennemann, Catalysis Communications 3 (2002) 565–571.
[39] H. Song, L.Z. Zhang, R.B. Watson, D. Braden, U.S. Ozkan, Catalysis Today 129 (2007) 346–354.
[40] U.S. Ozkan, H. Song, R.B. Watson, L.Z. Zhang, Abstracts of Papers of the American Chemical Society 231 (2006).
[41] J. Llorca, N. Homs, J. Sales, J.L.G. Fierro, P.R. de la Piscina, Journal of Catalysis 222 (2004) 470–480.
[42] J. Llorca, N. Homs, J. Sales, P.R. de la Piscina, Journal of Catalysis 209 (2002) 306–317.
[43] J. Llorca, P.R. de la Piscina, J.A. Dalmon, J. Sales, N. Homs, Applied Catalysis B: Environmental 43 (2003) 355–369.
[44] J. Llorca, J.A. Dalmon, P.R. de la Piscina, N. Homs, Applied Catalysis A: General 243 (2003) 261–269.
[45] S. Cavallaro, Energy & Fuels 14 (2000) 1195–1199.
[46] F. Can, A. Le Valant, N. Bion, F. Epron, D. Duprez, Journal of Physical Chemistry C 112 (2008) 14145–14153.
[47] H.S. Roh, A. Platon, Y. Wang, D.L. King, Catalysis Letters 110 (2006) 1–6.
[48] C. Ratnasamy, J.P. Wagner, Catalysis Reviews: Science and Engineering 51 (2009) 325–440.
[49] O. Gorke, P. Pfeifer, K. Schubert, Applied Catalysis A: General 360 (2009) 232–241.
[50] A. Platon, H.S. Roh, D.L. King, Y. Wang, Topics in Catalysis 46 (2007) 374–379.
[51] H. Song, U.S. Ozkan, Journal of Catalysis 261 (2009) 66–74.
[52] H. He, H.X. Dai, K.W. Wong, C.T. Au, Applied Catalysis A: General 251 (2003) 61–74.
[53] W. Cai, B. Zhang, Y. Li, Y. Xu, W. Shen, Catalysis Communications 8 (2007) 1588–1594.
[54] J. Kaspar, R. Di Monte, P. Fornasiero, M. Graziani, H. Bradshaw, C. Norman, Topics in Catalysis 16 (2001) 83–87.
[55] R.S. Murthy, P. Patnaik, P. Sidheswaran, M. Jayamani, Journal of Catalysis 109 (1988) 298–302.
[56] K. Takanabe, K.-i. Aika, K. Seshan, L. Lefferts, Chemical Engineering Journal 120 (2006) 133–137.
[57] Y. Zhang, K.J. Smith, Catalysis Today 77 (2002) 257–268.
[58] J.P. Pinheiro, M.C. Schouler, E. Dooryhee, Solid State Communications 123 (2002) 161–166.
[59] X.N. Li, Y. Zhang, K.J. Smith, Applied Catalysis A: General 264 (2004) 81–91.
[60] J.W. Snoeck, G.F. Froment, M. Fowles, Journal of Catalysis 169 (1997) 240–249.
[61] C.H. Bartholomew, Applied Catalysis A: General 212 (2001) 17–60.